Long-range correlations in low multiplicity pp collisions at $\sqrt{s} = 13.6$ TeV with ALICE

Olavi Kiuru[1]

Supervisors: Jasper Parkkila[2], Ivan Vorobyev[2]

August 18, 2023

Abstract

Current theoretical models do not predict the existence of collective-like effects in low multiplicity pp collisions. In this report, we show evidence for the existence of such collective-like effects using Run 3 data from the LHC. We obtain a ridge yield of $\mathcal{O}(10^{-4})$ for multiplicities in the range $15 - 20$.

[1]University of Helsinki, olavi.kiuru@helsinki.fi

[2]CERN

Contents

1 Introduction

The existence of collectivity in lead–lead (Pb–Pb) collisions has been studied extensively [1, 2]. In these collisions, the origin of the collectivity can be attributed to the fluid-like expansion of a quark-gluon plasma (QGP), created in the collision event shortly after thermalization. In contrast to regular hadronic matter, quarks and gluons are no longer confined in a QGP due to the extreme energy densities involved.

Recently, similar signatures of collectivity have been observed in high multiplicity collisions of smaller systems, i.e. proton–lead (p–Pb) and proton–proton (pp) collisions [3, 4]. However, the origin of these collective effects is not known, as the presence of a medium in small collision systems is not well established and other effects may play an important role [5].

To explain and reproduce the collective effects in simulations, new models were created [6–9]. Noteworthily, these models do not predict collectivity in low multiplicity pp collisions. With new data available from Run 3 of the Large Hadron Collider (LHC), the collective behaviour in low multiplicity pp collisions can be studied in more detail than before. If the presence of collectivity in low multiplicity pp collisions can be detected, it would suggest a gap in the current theoretical understanding of these events.

The structure of the report is the following. In section 2, the methods used to obtain the results are explained. In section 3, the results of the study are presented. Finally, in section 4, conclusions are drawn and and future outlooks are discussed.

2 Methods

In this section, the methods used to analyse the data are presented. For a more detailed explanation see [4]. The data used for the analysis is from a pp collision data set recorded by ALICE in 2022 as part of the Run 3 operation of the LHC. The data set included 966 221 600 same-event pairs and 4 713 617 000 mixed-event pairs.

2.1 Data selection

In the analysis, data from charged particles with transverse momenta $1.0 < p_{\mathrm{T}} < 2.0$ GeV/c and pseudorapidity $|\eta| < 1.0$ is used. The lower bound for the transverse momentum is chosen because for lower transverse momenta the detected jet peak is too wide for the analysis. The analysis is done separately for different multiplicity intervals of the collision events, where multiplicity is defined as the number of charged particles detected with $p_{\mathrm{T}} > 0.2$ GeV/c and $|\eta| < 1.0$.

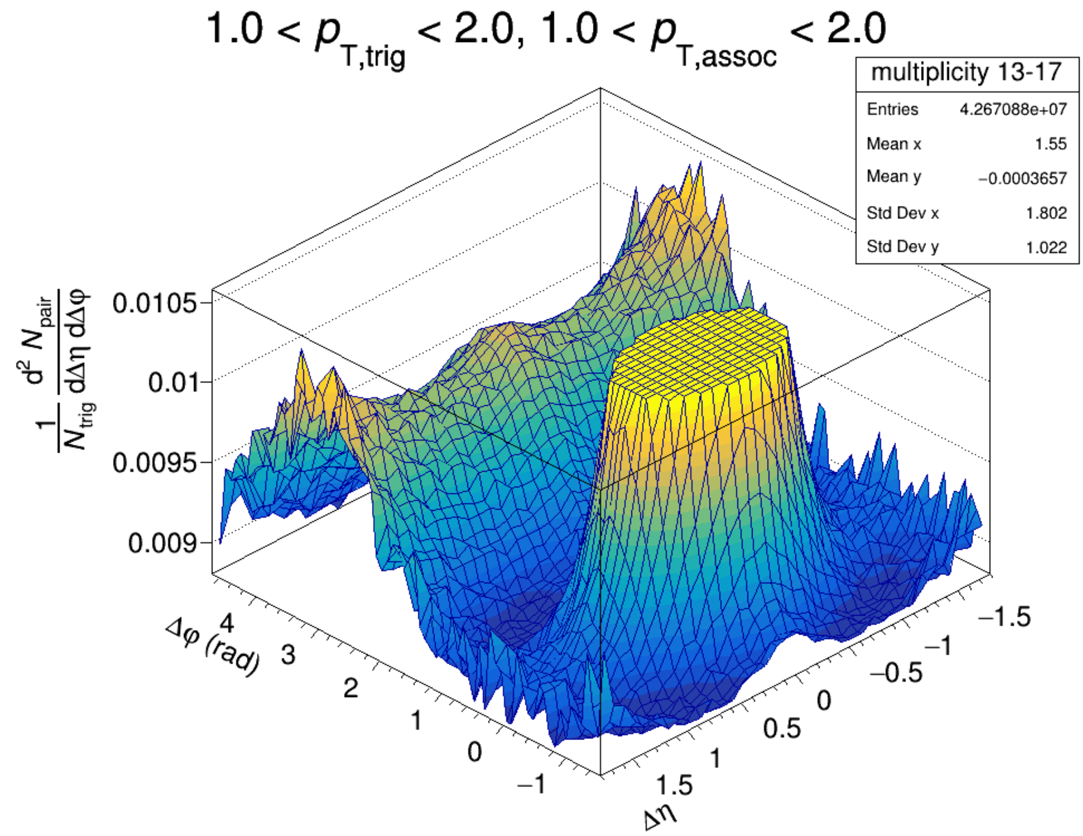

Figure 1: Two-particle correlation function for pp collisions with multiplicities in the range $12.750 - 17.750$.

For the tracking of the particles, the Inner Tracking System and Time Projection Chamber of the ALICE detector were used [1]. We will refer to multiplicities less than or equal to 20 as low multiplicities.

2.2 Analysis of experimental data

To quantify the amount of collectivity in a system, we define the two-particle correlation function

$$C(\Delta\eta, \Delta\varphi) = \frac{1}{N_{\text{trig}}} \frac{\mathrm{d}^2 N_{\text{pair}}}{\mathrm{d}\Delta\eta \mathrm{d}\Delta\varphi}, \tag{1}$$

where N_{trig} denotes the number of trigger particles, N_{pair} denotes the number of trigger-associated particle pairs, and $\Delta\eta$ and $\Delta\varphi$ denote the difference in pseudorapidity and azimuthal angle, respectively, between the trigger and associated particles. The correlation function is obtained by booking the $\Delta\eta$ and $\Delta\varphi$ of all particle combinations for each collision event into a same-pair distribution. The particles from the event are also paired with particles from a large event pool and booked into a mixed-pair distribution. This distribution is used to normalize the same-pair distribution to mitigate detector acceptance effects. The correlation function for collisions with multiplicities in the range $12.750 - 17.750$ is shown in Fig. 1.

The per-trigger yield is obtained by projecting the two-particle correlation function over the region $1.4 < |\Delta\eta| < 1.8$ and subtracting a constant offset C_{ZYAM} using the Zero-Yield-At-Minimum (ZYAM) procedure [10]. This $\Delta\eta$ range, often referred to as long range, has been chosen to minimize the contamination from the near-side ($\Delta\varphi \approx 0$) jet fragmentation peak.

The constant C_{ZYAM} is obtained by requiring that the per-trigger yield is zero evaluated at $\Delta\varphi = \Delta\varphi_{\mathrm{min}}$, where $\Delta\varphi_{\mathrm{min}}$ is the minimum of the third order Fourier cosine series fitted to the projected two-particle correlation function. Thus, the per-trigger yield is given by

$$\frac{1}{N_{\mathrm{trig}}}\frac{\mathrm{d}N_{\mathrm{pair}}}{\mathrm{d}\Delta\varphi} = \int_{1.4<|\Delta\eta|<1.8} C(\Delta\eta, \Delta\varphi)\frac{1}{\delta_{\Delta\eta}}\,\mathrm{d}\Delta\eta - C_{\mathrm{ZYAM}}, \tag{2}$$

where $\delta_{\Delta\eta} = 0.8$ is a normalisation factor.

Finally, the ridge yield Y^{ridge} is obtained by integrating over the near-side peak of the projection:

$$Y^{\mathrm{ridge}} = \int_{|\Delta\varphi|<|\Delta\varphi_{\mathrm{min}}|} \frac{1}{N_{\mathrm{trig}}}\frac{\mathrm{d}N_{\mathrm{pair}}}{\mathrm{d}\Delta\varphi}\,\mathrm{d}\Delta\varphi\,. \tag{3}$$

2.3 Efficiency corrections

The measured multiplicity by the detectors does not perfectly match reality due to various detector effects. To account for these detector effects, Monte Carlo (MC) simulations are used. With the MC simulations we can estimate the impact of the detector effects and use this estimate to correct the measured data.

There are two types of corrections that need to be applied. First, a correction to the measured multiplicities is applied. For this we use MC data to estimate how many particles the detector misses. The corrections given by the MC data are shown in Fig. 2a. The effect of the multiplicity correction is to shift the measured ridge yield curve towards higher multiplicities.

Second, corrections need to be applied to the measured ridge yield value. The effect of this correction is to shift the measured ridge yield to higher values. The efficiency predicted by the MC data is shown in Fig. 2b.

The validity of the efficiency corrections is tested in the following way. First, a MC data set is created assuming a perfect detector. We call this data set "MC

(a) (b)

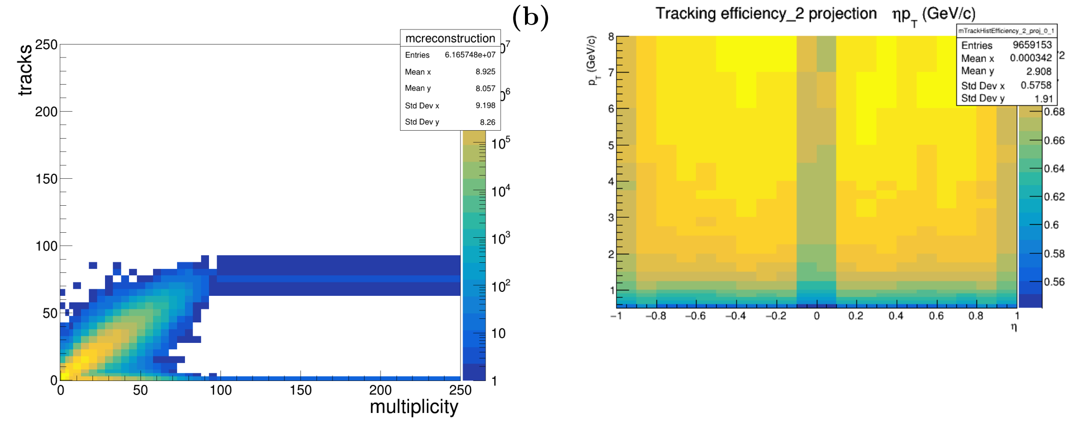

Figure 2: a) MC data used for correcting the measured multiplicities. The measured value of the multiplicity is given on the y-axis and the true value on the x-axis. b) Measured efficiency as a function of transverse momenta and pseudorapidity.

truth". Detector effects are then applied to the data set and this more realistic data set is analyzed. The results from this analysis are referred to as "reconstructed". Afterwards, efficiency corrections are applied to the reconstructed result to obtain the "corrected" result. If the efficiency corrections work properly, the corrected result should match the MC truth result. Fig. 3 shows the results of this test.

The ratio of the corrected result and the MC truth result is close to one for all relevant multiplicities. From this we can conclude that the efficiency corrections are working as intended. The results shown here were calculated on the away-side ($\Delta\varphi \approx \pi$) ridge due to problems in the near-side MC data.

3 Results

In this section, the results of the summer project are presented. The effect of systematic uncertainty on the result is also discussed, as well as future plans for improving the results.

3.1 Ridge yield

Fig. 4a shows the obtained ridge yield from Run 3 data. The original experimental data is shown in blue and the efficiency corrected data in red. The ridge yield is non-zero within error bars down to a multiplicity of 10. A comparison between Run 2 [11] and Run 3 results is shown in Fig. 4b. Here, the Run 3 data is shown in blue and the Run 2 data in red. The results from the two runs are consistent

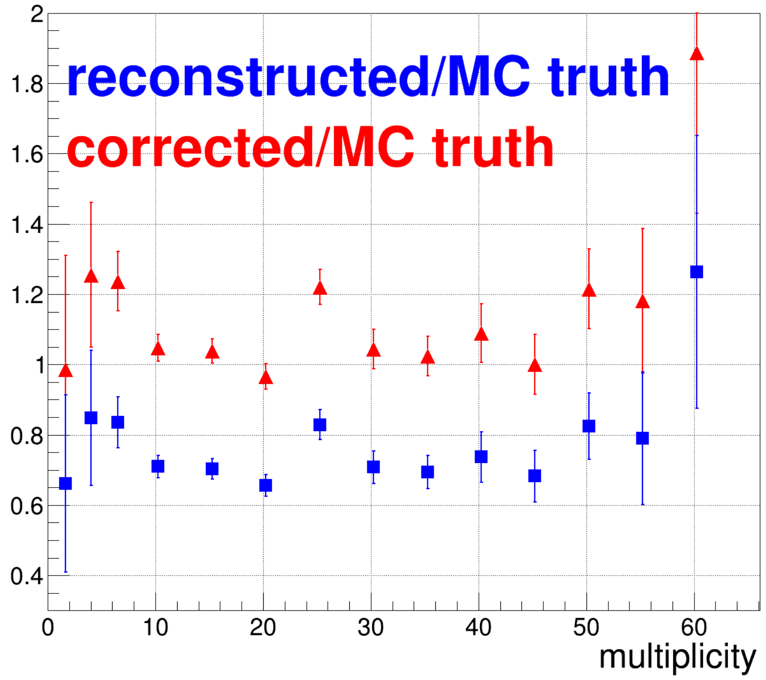

Figure 3: Validity test of the efficiency corrections. The ratio of the reconstructed data and the ideal MC data is shown in blue and the ratio between the corrected data and the ideal MC data is shown in red. The results of the plot are from the away-side ridge of the MC data.

within the errors given for low multiplicities. For multiplicities in the range $15-20$, the ridge yield is of the order $\mathcal{O}(10^{-4})$.

Sources	Systematic uncertainty (%)
$\Delta\eta$ interval	$\pm 0.3 - 45\%$
$\Delta\varphi$ integration bounds	$\pm 1.8 - 39\%$
Wing correction	$\pm 5.1 - 41\%$
Total (in quadrature)	$\pm 6.6 - 62\%$

Table 1: Systematic uncertainty in the calculation of the ridge yield. The details of the calculation are presented in Sec. 3.2.

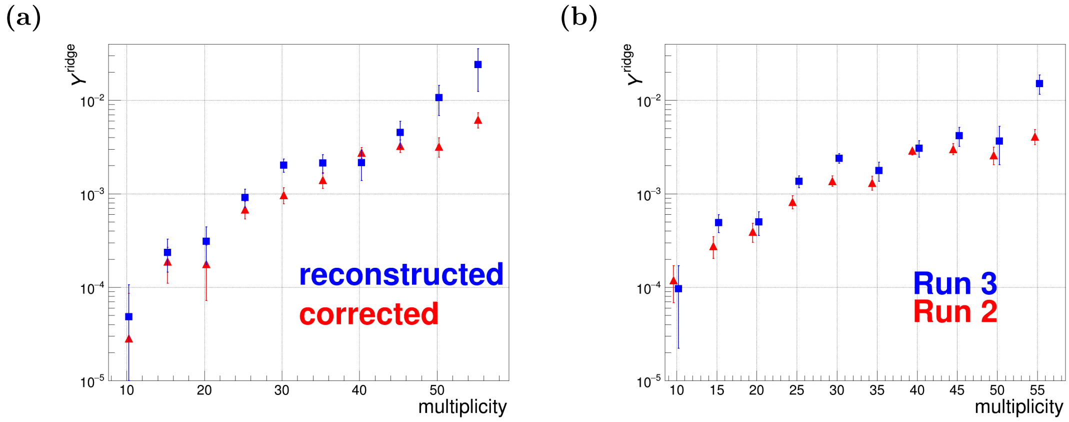

Figure 4: a) Ridge yield of pp collisions as a function of multiplicity. The blue squares show the resulting ridge yield calculated based on the experimental data and the red triangles show the result after applying MC efficiency corrections to the measured data. b) Comparison between Run 2 and Run 3 results. Run 2 is shown in red and Run 3 in blue.

3.2 Systematic uncertainty

To estimate the impact of various detector effects and experimental choices on the results, we evaluate the systematic uncertainty. This is done by changing some parameter in the calculation and seeing how much the result changes compared to the original calculation. The results of this calculation are presented in Table 1.

To estimate the remaining contributions from the near-side jet fragmentation peak, the lower integration bound of $\Delta\eta$ in Eq. (2) was changed from 1.4 to 1.5. The effect of the $\Delta\varphi$ integration bounds was estimated by shifting the integration bounds in Eq. (3) by one histogram bin to the right. The two-particle correlation function shown in Fig. 1 shows an upward bend at large values of $|\Delta\eta|$. This upward bend is often referred to as the wings of the correlation function and is caused by residual two-particle acceptance effects. The systematic uncertainty due to the wings can be obtained through a more involved calculation that is beyond the scope of this report.

There are further effects that cause systematic uncertainty in the value of the ridge yield. For a more detailed explanation of systematic errors, see [4]. The total systematic uncertainty is obtained by adding up all individual forms of systematic uncertainty in quadrature.

(a) (b)

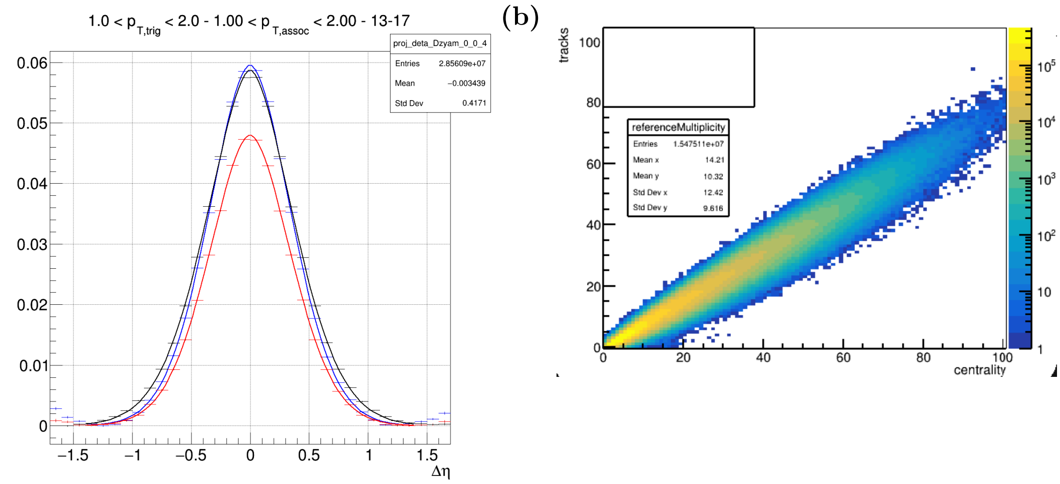

Figure 5: a) The $\Delta\eta$ projection of the two-particle correlation function. The reconstructed result is shown in red, the corrected result in blue and the Run 2 result in black. A generalized Gaussian distribution is fitted to each data set. An unphysical upward bend is present at the edges of the distribution. b) Multiplicity corrections from Run 2 MC data.

3.3 Future improvements

In this section, some improvements to the analysis are suggested, to increase the precision of the obtained result.

As discussed above, the measured two-particle correlation function bends upward at large $\Delta\eta$. This is most clearly seen in the $\Delta\eta$ projection of the correlation function, shown in Fig. 5a. In the figure, the corrected result is shown in blue, the reconstructed result in red and the Run 2 result in black. The bend is most likely due to residual acceptance effects in the detector. In future work, corrections should be applied to the data to mitigate the effect of these residual acceptance effects on the result.

There are also some issues with the MC data used in the analysis. In Fig. 2a, the multiplicity correction given by the Run 3 MC data is shown. There are many particles with small track values but large multiplicity values. This should not happen and can most likely be attributed to the work-in-progress nature of the Run 3 MC corrections. The corrections should be similar to those used for Run 2, shown in Fig. 5b.

Additionally, only a subset of the available Run 3 data was used. Making use of all of the available data would give a more accurate result.

4 Conclusions

In this report, new data from Run 3 of the LHC was used to study collectivity in low multiplicity pp collisions. The results show evidence for the existence of collectivity in the system. The obtained ridge yield of $\mathcal{O}(10^{-4})$ for multiplicities in the range $15 - 20$ is consistent with earlier calculations on LHC Run 2 data. This is significantly larger than the ridge yield measured from an electron-positron (e^+e^-) annihilation system [12], indicating a prominent contribution to collectivity from mechanisms not present in e^+e^- collisions.

However, more data is needed to reduce the uncertainty of the results obtained. More work is also needed to mitigate the effects of systematic uncertainties on the result and to fix some of the issues both in the collected data and the MC data. If the existence of collectivity in low multiplicity pp collisions is confirmed, new theoretical work is required to understand its origin.

Acknowledgements

I would like to thank my supervisors, especially my main supervisor Jasper Parkkila, for their invaluable help during this project. I would also like to thank CERN and everyone involved in organizing the 2023 Summer Student Programme for this incredible opportunity and all the interesting lectures and workshops that I had the chance to attend. Finally, I would like to thank all my friends, both new and old, for making this summer the best summer of my life.

References

[1] ALICE Collaboration. *The ALICE experiment – A journey through QCD*. arXiv:2211.04384 [hep-ex, physics:nucl-ex]. 2022. DOI: 10.48550/arXiv.2211.04384.

[2] Wit Busza, Krishna Rajagopal, and Wilke van der Schee. "Heavy Ion Collisions: The Big Picture, and the Big Questions". In: *Annual Review of Nuclear and Particle Science* 68.1 (2018). arXiv:1802.04801 [hep-ph, physics:hep-th, physics:nucl-ex, physics:nucl-th], pp. 339–376. ISSN: 0163-8998, 1545-4134. DOI: 10.1146/annurev-nucl-101917-020852.

[3] I G Altsybeev and for the ALICE collaboration. "Long-range correlations in ALICE at the LHC". In: *Journal of Physics: Conference Series* 798.1 (2017), p. 012056. DOI: 10.1088/1742-6596/798/1/012056.

[4] ALICE Collaboration. "Long- and short-range correlations and their event-scale dependence in high-multiplicity pp collisions at $\sqrt{s} = 13$ TeV". In: *Journal of High Energy Physics* 2021.5 (2021). arXiv:2101.03110 [hep-ex, physics:nucl-ex], p. 290. ISSN: 1029-8479. DOI: 10.1007/JHEP05(2021)290.

[5] J. L. Nagle and W. A. Zajc. "Small System Collectivity in Relativistic Hadron and Nuclear Collisions". In: *Annual Review of Nuclear and Particle Science* 68.1 (2018). arXiv:1801.03477 [hep-ph, physics:nucl-ex, physics:nucl-th], pp. 211–235. ISSN: 0163-8998, 1545-4134. DOI: 10.1146/annurev-nucl-101916-123209.

[6] Christian Bierlich, Gösta Gustafson, and Leif Lönnblad. "Collectivity without plasma in hadronic collisions". In: *Physics Letters B* 779 (2018), pp. 58–63. ISSN: 0370-2693. DOI: https://doi.org/10.1016/j.physletb.2018.01.069.

[7] Mao-Wu Nie et al. "Multiparticle azimuthal cumulants in $p+$Pb collisions from a multiphase transport model". In: *Phys. Rev. C* 98 (3 2018), p. 034903. DOI: 10.1103/PhysRevC.98.034903.

[8] P. Romatschke. "Collective flow without hydrodynamics: simulation results for relativistic ion collisions". In: *The European Physical Journal C* 75.9 (2015), p. 429. ISSN: 1434-6052. DOI: 10.1140/epjc/s10052-015-3646-8.

[9] Ryan D. Weller and Paul Romatschke. "One fluid to rule them all: Viscous hydrodynamic description of event-by-event central p+p, p+Pb and Pb+Pb collisions at s=5.02 TeV". In: *Physics Letters B* 774 (2017), pp. 351–356. ISSN: 0370-2693. DOI: https://doi.org/10.1016/j.physletb.2017.09.077.

[10] N. N. Ajitanand et al. "Decomposition of harmonic and jet contributions to particle-pair correlations at ultrarelativistic energies". In: *Phys. Rev. C* 72 (1 2005), p. 011902. DOI: 10.1103/PhysRevC.72.011902.

[11] J. E. Parkkila. *Long-range correlations in low-multiplicity pp collisions at* $\sqrt{s} = 13\,\text{TeV}$. 2023. arXiv: 2306.04808 [nucl-ex].

[12] Anthony Badea et al. “Measurements of Two-Particle Correlations in e^+e^- Collisions at 91 GeV with ALEPH Archived Data”. In: *Phys. Rev. Lett.* 123 (21 Nov. 2019), p. 212002. DOI: 10.1103/PhysRevLett.123.212002. URL: https://link.aps.org/doi/10.1103/PhysRevLett.123.212002.